Enhanced responsivity of β-Ga_2O_3 ultraviolet photodetector using Pt/ ITO stacked electrode

FENG LIN[a], LEI YUAN[a,*], HONGPENG ZHANG[a], JIANGANG YU[a], XIAOYAN TANG[a], XIAOZHENG LIAN[b], SHENGNAN ZHANG[b], HONGJUAN CHENG[b], JICHAO HU[c], YIMEN ZHANG[a], YUMING ZHANG[a], RENXU JIA[a]
[a]*Wide Bandgap Semiconductor Technology Disciplines State Key Laboratory, Xidian University, Xi'an 710071, China*
[b]*China Electronics Technology Group Corporation No. 46 Research Institute, Tianjin 300220, China*
[c]*Department of Electronic Engineering, Xi'an University of Technology, Xi'an 710048, China*

In this paper, 10 nm Pt / 90 nm ITO stacked electrode was employed to form the MSM-structured β-Ga_2O_3 UV photodetectors, for comparison with the detectors using single 100 nm Pt electrodes. The optical response characteristics were mainly studied, and it was found that the photocurrent and responsivity of the β-Ga_2O_3 detector using the Pt/ITO electrode is almost 1000 times that of the Pt electrode detector, which is due to the higher light transmittance of the Pt/ITO stacked layers. The results of the experiment indicate that the Pt/ITO stacked electrode is helpful for enhancing the performance of β-Ga_2O_3 UV photodetectors.

(Received April 20, 2020; accepted November 25, 2020)

Keywords: Ga_2O_3, Solar blind UV detector, Optical responsivity, Light-dark current ratio, Transient response

1. Introduction

Ultraviolet detection technology has broad application prospects in several applications, such as missile tail flame, ozone hole monitoring and optical communication, which has attracted more and more attention and research. Generally, the ultraviolet spectrum could be divided into four different types according to its wavelength range, including UV-A (315 nm to 400 nm), UV-B (280 nm to 315 nm), UV-C (200 nm to 280 nm) and VUV (10 nm to 200 nm) [1]. Among them, the range of 200 nm to 280 nm is strongly absorbed by the ozone sphere, which is difficult to propagate to the earth, also called "solar blind ultraviolet". Thus, the sunlight makes little interference with the solar blind ultraviolet detectors.

To obtain the solar blind ultraviolet detector with superior performance, semiconductor materials with band gap greater than 4.4 eV is the best choice, such as AlGaN (3.4-6.2 eV) [2,3], MgZnO (3.3-7.8 eV) [4], diamond (5.5 eV) [5,6] and Ga_2O_3 (4.4-5.3 eV) [7-10]. The band gap of AlGaN and MgZnO can be changed by adjusting the composition of aluminum and magnesium, respectively. However, increasing the composition of the doped metal will cause significant degradation of the film quality of these two materials [11-13]. Diamond has a suitable band gap, but the basic semiconductor tunable spectral response range is limited, and the lack of large-area single crystal also limits the practical application of this material. In recent years, Ga_2O_3 materials have received a lot of attention for its suitable band gap width (4.4-5.3 eV) and mature preparation process. There are already some methods for growing large-sized Ga_2O_3 substrates, and they are cheap. At present, there have been many reports of solar blind UV detectors based on Ga_2O_3 single crystals, films, and nanostructures. In 2017, Cui et al reported a MSM-type Ga_2O_3 solar blind photodetector. By controlling the oxygen flux during the growth of the Ga_2O_3 amorphous film, the oxygen vacancy of the active layer is reduced, so the sample has higher resistance, low dark current and fast decay rate [14]. In 2019, Han et al reported a high-performance Ga_2O_3 photodetector with MSM structure. They found that the detector prepared by the Ga_2O_3 thin film deposited under the Ar pressure of 0.5Pa has the highest photoresponsivity. The maximum response of the device reached 436.3 A/W under 240 nm UV light with a 25 V bias voltage [15]. In 2020, Vu et al reported a MSM structure Ga_2O_3 photodetector. By controlling the oxygen partial pressures from 0 to 50 mTorr when depositing the β-Ga_2O_3 thin film, they prepared an ultraviolet detector, which reached a highest photoresponsivity of 5 A/W under the condition of 258 nm ultraviolet illumination and 25 V bias [16].

The MSM (metal-semiconductor-metal) structure is a commonly used ultraviolet detector structure. By depositing a metal interdigital electrode on a semiconductor substrate, two coherent Schottky junctions are formed back-to-back, and the incident light is absorbed in the gap between the metal interdigital electrodes [14]. However, due to the serried electrodes, the optical area is reduced, which seriously affects the photoelectric

performance of the detector. To solve this, one feasible method is to increase the incident amount of light per unit area. Using transparent conductor, such as ITO (Indium Tin Oxide) as the electrode of the MSM detector can increase the incident amount of light [17]. ITO is the most widely used and widely used transparent conductive material. The work function of ITO is 4.5-4.9 eV (smaller than the work function of Ga_2O_3), which makes it difficult to form a Schottky contact between ITO and Ga_2O_3. A low barrier height will lead to a high Leakage current, which will affect the performance of the detector. In this paper, the Pt/ITO stack electrode structure is used to enhance the photoelectric performance of the detector. 10 nm Pt and 90 nm ITO was grown on a β-Ga_2O_3 (100) single crystal substrate to fabricate the photodetector. Another photodetector depositing 100 nm Pt as an electrode was fabricated for comparison. By studying the photoelectric characteristics of the detector, the feasibility of using Pt/ITO structure electrodes to enhance the photoresponsivity of the detector was verified.

2. Experiment

N-type β-Ga_2O_3 (100) single crystal material is used as the substrate of the detector. The crystal is fabricated by CETC 46th institute using the Edge-defined Film-fed Growth (EFG) method with silicon doping concentration of 10^{18} cm^{-3} and the surface roughness less than 0.5 nm. All β-Ga_2O_3 substrates used in this experiment was cut from the same crystal. XRD (X-ray diffraction) analysis and UV-vis (ultraviolet spectrophotometer) test were performed to determine the crystal quality and composition of the material. The substrate was cleaned before the electrode's deposition. First, the single wafer was washed with acetone, absolute ethanol, and deionized water for 10 minutes, and then the wafer was blown dry with nitrogen. The purpose of these steps was to remove impurity ions and contamination on the surface of the wafer.

Photolithography is used on the surface of the substrate to form the interdigital electrodes. The process flow is shown in Fig. 1. A too thick metal layer will affect the light transmittance of the Pt/ITO electrode, so we decided to grow a 10 nm thick Pt layer. Using a DC magnetron sputtering, a 100 nm Pt metal layer and a 10 nm/90 nm Pt/ITO layer were separately deposited on the front surface of the lithographic single crystal substrate. The sputtering process was carried out under Ar atmosphere and room temperature conditions. When sputtering ITO, the sputtering power was set to 25 W, and the deposition rate was about 2.3 nm/min, and it takes 2314 s to sputter 90 nm ITO film. After the sputtering was completed, the sample was immersed in an acetone solution and then subjected to stripping by means of ultrasonic cleaning. For convenience, the gallium oxide ultraviolet detector with a Pt electrode is simply referred as the detector 1, and the gallium oxide detector with a Pt/ITO electrode is simply referred as the detector 2. The 254 nm/365 nm optional UV lamp was used as the light source, and the test power density was adjusted to 2.0 mW/cm^2 calibrated by commercial UV enhanced silicon photodetector (Newport 818) and power meter (Newport 841). The detector was tested by the Keithley-1500A and Cascade EPS150 probe station.

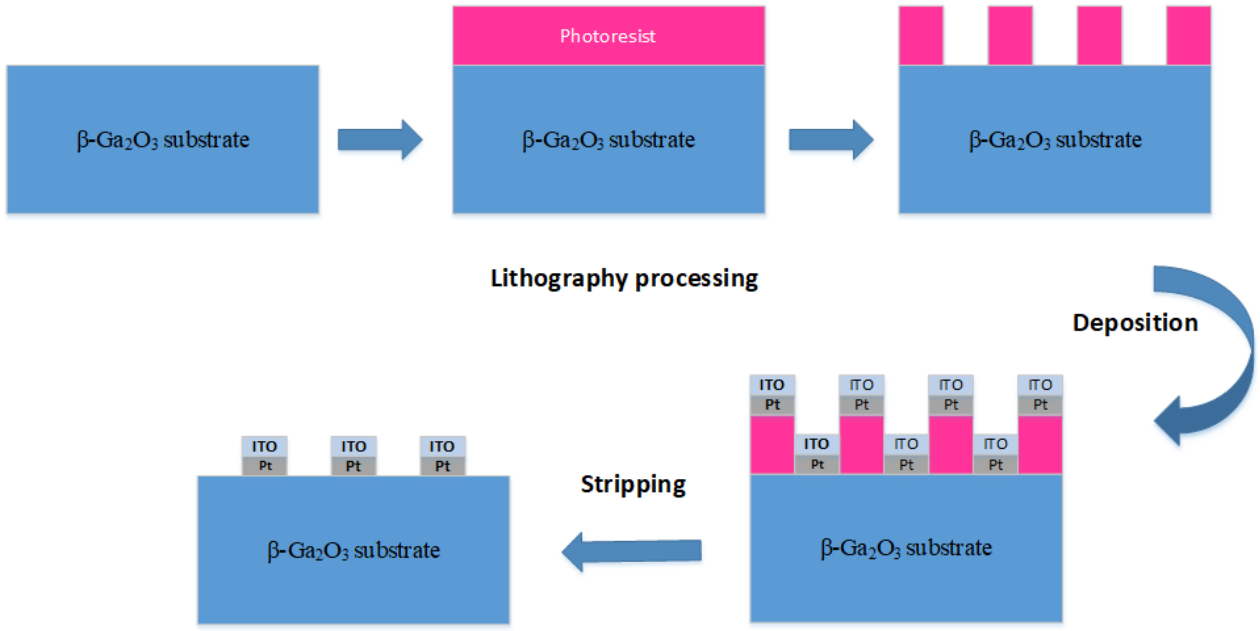

Fig. 1. The process of fabricating MSM structure detector (color online)

3. Results and discussion

In order to determine the crystal quality and composition of the substrate, a large-scale 2θ scan from 10 ° to 80 ° was performed, and the XRD pattern obtained is shown in Fig. 2(a). It can be seen that the three diffraction peaks of the single crystal material appear at three positions of 30.06 °, 45.98 ° and 62.55 °, which correspond to the (400), (600), and (800) planes of β-Ga_2O_3 [18,19]. This result indicates that the β-Ga_2O_3 sample has good orientation in the (100) crystal direction. There are no diffraction peaks of other impurities in the XRD pattern, and the three diffraction peaks of β-Ga_2O_3 have high intensity, indicating that the sample has high purity and good crystal quality. The absorption spectrum of the β-Ga_2O_3 material was obtained by an UV–Vis spectroscopy test (Fig. 2b). It can be seen from the absorption spectrum that a steep absorption edge appears at the boundary of the solar blind ultraviolet region, which is consistent with the direct band gap transition characteristics of gallium oxide [20]. The band gap of the gallium oxide material can be calculated as 4.72 eV by the Tauc Plot method (shown in the insert of Fig. 2b).

In order to obtain the performance parameters of the two devices, the I-V (current-voltage) characteristic curves in both the dark and 254 nm illumination was measured, with the applied voltage range of -8 to 8 V and a voltage step of 0.05 V. The logarithmic coordinate system is used in Fig. 3 to better compare the photocurrent and dark current of the two detectors, and the insert is the I-V curve in linear coordinate system.

It can be seen from Fig. 3 that the photocurrent of the detector1 is only reaches the order of 10^{-7} A at a bias voltage of 8 V, and the photocurrent of the detector2 reaches the order of 10^{-5} A, which is hundreds of times of the former. The corresponding optical responsivity is remarkably improved. It can be seen that the dark current of the detector 2 also has a rise compared to the detector 1, reaching the order of 10^{-8}A. Higher dark current can be attributed to the poor quality of thin metal layers. The process optimization of this kind of metal stack is not enough, and such a thin metal film grown by magnetron sputtering is not uniform enough, which may cause local contact between ITO layer and Ga_2O_3 substrate. However, this problem can be solved by further parameter adjustments, such as the control of power and cavity pressure. This article focuses on the light response characteristics.

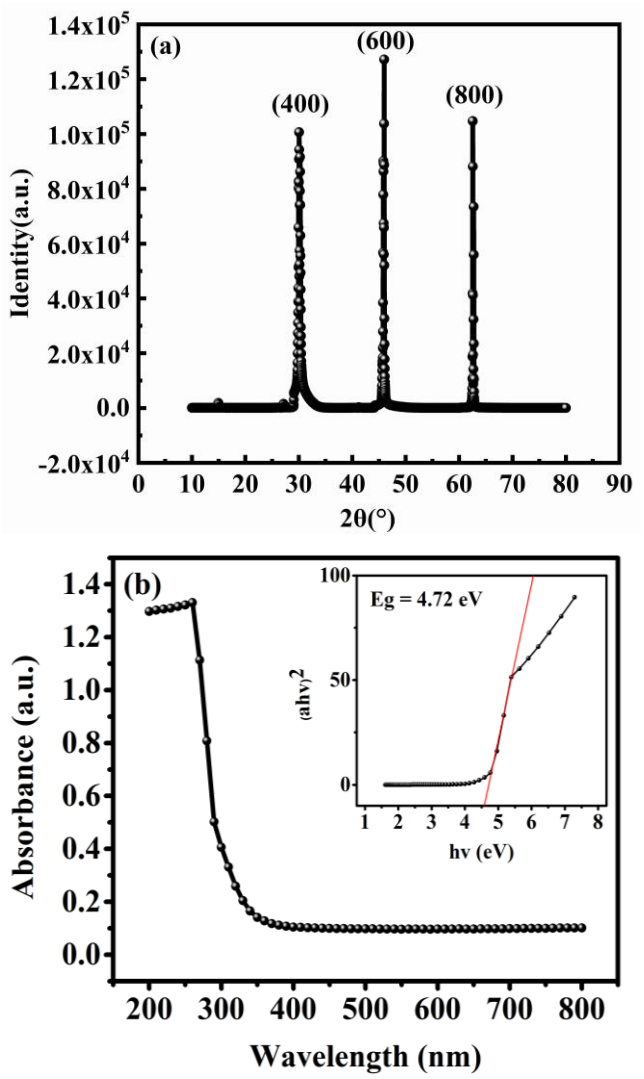

Fig. 2. (a) XRD pattern of gallium oxide single crystal material. (b) Absorption spectrum of gallium oxide single crystal material

Although the dark current of detector 2 is increased compared to that of detector1, the increase in photocurrent makes the ratio of light and dark current of detector 2 not significantly reduced. To make a more intuitive comparison of the two different detectors, the light-dark current ratio curves was put together, as shown in Fig. 4(a). It can be found from the figure that when the bias voltage is greater than 2 V, the light-dark current ratio of the two detectors changes smoothly (show a trend of rising first and then falling), and their numerical difference is very small (when they have the largest difference, the larger value is still only twice the smaller value). In the interval of 4-6.8 V, the light-dark current ratio of both detectors is more than 1000, and the dark current of detector 2 is larger than that of detector 1.

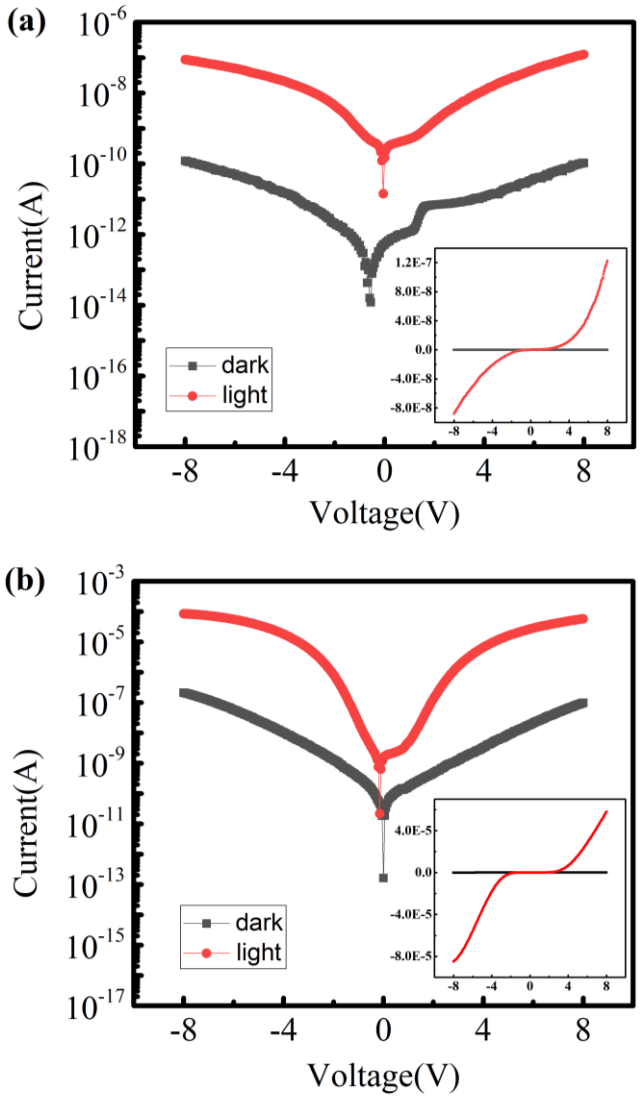

Fig. 3. (a) The current voltage (I-V) characteristics of the detector1 in dark, and 254 nm illumination. (b) The current voltage (I-V) characteristics of the detector 2 in dark, and 254 nm illumination (color online)

Fig. 4(b) shows the responsivity-voltage curves of the two detectors in logarithmic coordinate system of the two UV photodetectors. The calculation of the responsivity is obtained by the following formula [10]

$$R = \frac{I_{ph} - I_{dark}}{P_\lambda S} \quad (1)$$

where I_{ph} is the photocurrent, I_{dark} is the dark current, P_λ is the optical power density, and S is the effective illumination area. The effective illumination area of these devices is 5.23×10^{-4} cm^2, and the optical power density used in the experiment was 2.0 mW/cm^2, so the responsivity of the detectors can be calculated using the above formula based on the experimental test results. At a bias voltage of 4.1 V, the light-dark current ratio of the detector 2 reaches a peak value of 2.04×10^3, and the oresponsivity of the detector 2 is 7.05 A/W, while the responsivity of the detector1 is 0.01 A/W; at a bias voltage of 4.6 V, the light-dark current ratio of the detector1 reaches the peak value of 1365, which is lower than the peak value of the detector2, and the responsivity of the detector 1 is only 0.02 A/W, while the detector 2 has a responsivity of 11.25 A/W. At a bias voltage of 8 V, the responsivity of the detector1 is still only 8.40×10^{-2} A/W, and the responsivity of the detector 2 reaches 81 A/W, which is nearly a thousand times higher than the former.

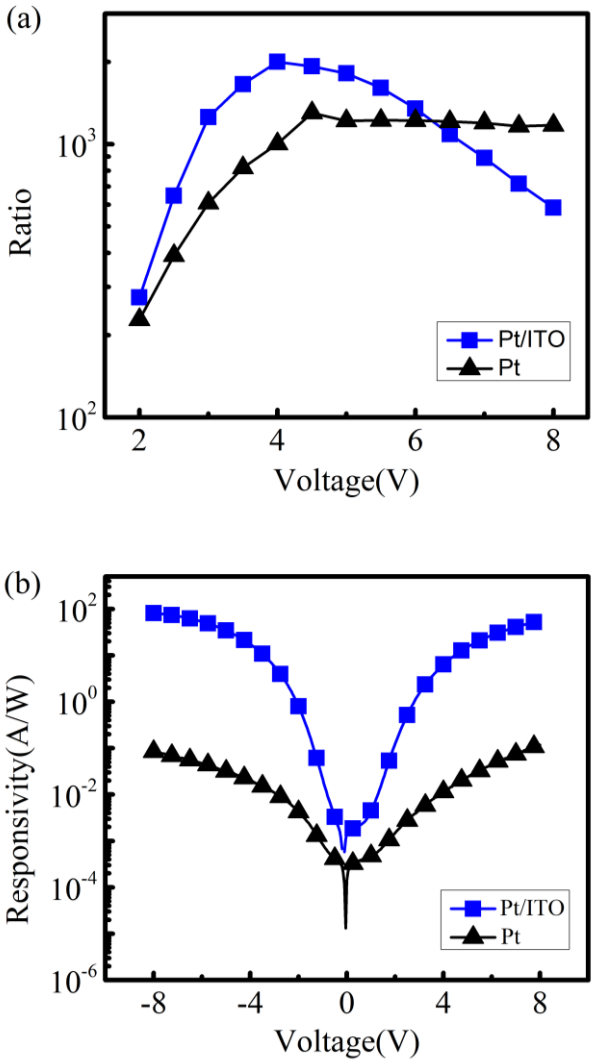

Fig. 4. (a) Light-dark current ratio of two detectors. (b) Photoresponsivity of two detectors (color online)

The photoresponsivity of detector 2 we prepared reaches 81 A/W under 254 nm UV light with a 8 V bias voltage, while that reported by Han et al. was 50 A/W under 240 nm UV light with a 10 V bias voltage [15], and that by Vu et al. was 5 A/W under 254 nm UV light with a 25 V bias voltage [16], so the detector we prepared has some advantages in performance.

The detectivity D is a parameter describing the ability

of detector to detect the minimum signal. For photodetectors, a higher detectivity indicates a better ability to detect the minimum optical signal. The detectivity *D* can be expressed as

$$D = \sqrt{\frac{SR^2}{2eI_{dark}}} \tag{2}$$

At a bias voltage of 8 V, the detector 1 has a detectivity of 3.08×10^{11} cm·Hz$^{1/2}$·W^{-1}, while the detector 2 has a detectivity of 7.10×10^{12} cm·Hz$^{1/2}$·W^{-1}, which is higher than the former.

Since the results of typical devices may be contingent, we tested and compared the photocurrent of all MSM-type detectors in two cells on two samples to avoid the contingency, and the results are shown in Fig. 5. Obviously, the photocurrent of the detectors with Pt/ITO electrodes is generally much larger than that of the Pt electrode UV detector, so the corresponding photoresponsivity is also much larger, which indicates that the Pt/ITO electrode can greatly increase the responsivity of the device in the ultraviolet band. Based on this result, the dark current of the Pt / ITO stacked electrode Ga_2O_3 solar blind UV detector can be further reduced by optimizing the metal deposition process and the overall performance of the device, such as adding a annealing process to improve the quality of metal film, thereby further improving light-dark-current ratio, detectivity, etc.

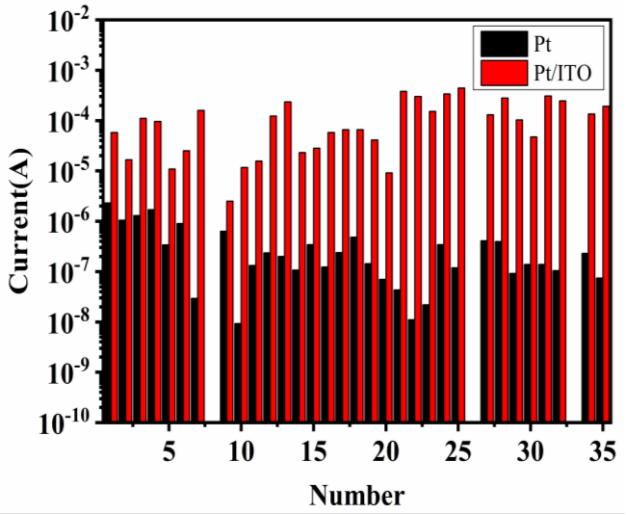

Fig. 5. The photocurrent of all 35 groups of devices at 8V (color online)

The transient response characteristics curve of the detector 2 has been tested using a Keithley-1500A probe station (the 254 nm UV lamp is switched on/off every 15 seconds, and the total time of test is 170 s), and the result is shown in Fig. 6. It can be seen that the two detectors have typical transient response curves, and detector 2 reaches the peak photocurrent faster than detector 1.

However, the response speed of these two detectors is slow, which indicates that there is a serious PPC effect inside the device (Persistent Photoconductivity) [21,22,23]. According to the literature, when the material is illuminated, its conductivity will increase rapidly, and as the duration of illumination increases, the growth rate of the photoconductive will slow down; after stopping the illumination, the conductance will decrease rapidly, and as the duration of stopping illumination increases, the decay rate of the photoconductive becomes slower and cannot be restored to the state before illumination, which is called the PPC effect. The PPC effect appearing in this experiment can be attributed to the low-resistance single crystal we use. The doped element Si inside the crystal may bring some additional defects, and these defects serve as traps for trapping photo-generated holes, which exacerbates the PPC effect [21]. Obviously, under the PPC effect, Fig. 6(b) shows a light-dark current ratio of 2, which is much lower than that shown in Fig. 4(a). Reducing the defect density of the active layer is an important method to solve this problem. The oxygen vacancies can be reduced by further annealing in an oxygen atmosphere [24].

It can be seen that the transient response curve of the detector is smooth and has good periodicity. The photocurrent of the detector has reached a maximum value since the third test cycle. The transient response characteristics of the photodetector were studied by double exponential relaxation function fitting. The function is expressed as [10,14,24]

$$I = I_0 + A_1 e^{(t-t_0)/\tau_1} + A_2 e^{(t-t_0)/\tau_2} \tag{3}$$

where I_0 is the steady current value when applying or removing illumination, A_1 and A_2 are constants, t_0 is the starting value of the fitting interval, and τ_1 and τ_2 are the fast-response component and the slow-response component. The fast-response component is attributed to the rapid change of the carrier concentration inside the device when the light-dark state is switched, while the slow response component is attributed to the carrier trapping/releasing due to the presence of trapping defects. The fitting result is shown in Fig. 6(c). The rise time of the photodetector with a Pt/ITO electrode is (0.34 s/0.34 s), the decay time is (0.39 s/4.91 s), and the slow decay component reaches 4.91 s, which reflects the PPC effect caused by the deep level defects trapping carriers [23,25].

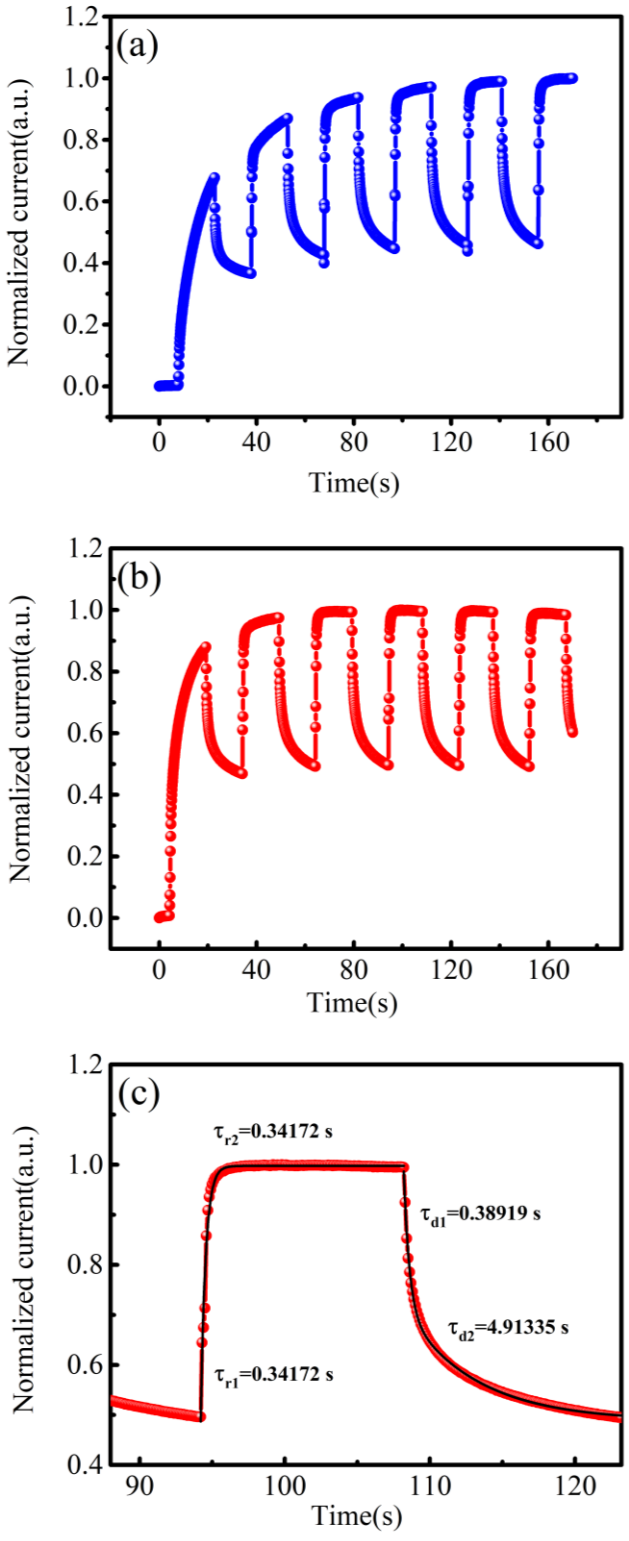

Fig. 6. (a) Normalized transient response curve of the detector 1. (b) Normalized transient response curve of the detector 2. (c) Fitting result of single-period transient response curve of the detector 2.

4. Conclusion

In this paper, two kinds of β-Ga_2O_3 solar blind UV photodetectors with Pt electrode and Pt/ITO electrode were fabricated, and their static and dynamic properties of the light and dark environment are studied. Experiments have shown that the Pt/ITO electrode can effectively improve the photoresponsivity of the UV detector while maintaining the same level of light-dark current ratio as the Pt electrode UV detector. This is because the Pt/ITO translucent electrode can effectively increase the amount of light incident on the surface of the active layer of the ultraviolet detector. The above experimental results show that the UV detector with Pt/ITO electrode has some advantages over that with pure Pt electrode, which is an effective method to improve the performance of UV detector.

Acknowledgement

This work is supported by the National Natural Science Foundation of China (Grant No. 61874084, 61704125 and 61904146), the Fundamental Research Funds for the Central Universities (Grant No. XJS191102), the Natural Science Foundation of Shaanxi Province, China (Grant No.2020JQ-302) and the Innovation Fund of Xidian University.

References

[1] E. Monroy, F. Omns, F. Calle, Semicond. Sci. Tech. **18**(4), R33 (2003).
[2] D. Li, K. Jiang, X. Sun, C. Guo, Adv. Opt. Photonics **10**(1), 43 (2018).
[3] Z. G. Shao, D. J. Chen, H. Lu, R. Zhang, D. P. Cao, W. J. Luo, Y. D. Zheng, L. Li, Z. H. Li, IEEE Electron Device Lett. **35**(3), 372 (2014).
[4] J. Yu, C. X. Shan, J. S. Liu, X. W. Zhang, B. H. Li, D. Z. Shen, Phys. Status Solidi RRL **7**(6), 425 (2013).
[5] S. Salvatori, M. C. Rossi, F. Galluzzi, E. Pace, Mater. Sci. Eng. B **46**(1-3), 105 (1997).
[6] Y. C. Chen, Y. J. Lu, C. N. Lin, Y. Z. Tian, C. J. Gao, L. Dong, C. X. Shan, J. Mater. Chem. C **6**(21), 5727 (2018).
[7] T. Onuma, S. Saito, K. Sasaki, T. Masui, T. Yamaguchi, T. Honda, M. Higashiwaki, Jpn. J. Appl. Phys. **54**(11), 112601 (2015).
[8] K. Akaiwa, S. Fujita, Jpn. J. Appl. Phys. **51**(7), 070203 (2012).
[9] S. Fujita, M. Oda, K. Kaneko, T. Hitora, Jpn. J. Appl. Phys. **55**(12), 1202a1203 (2016).
[10] D. Y. Guo, Y. L. Su, H. Z. Shi, P. G. Li, N. Zhao, J. H. Ye, S. L. Wang, A. P. Liu, Z. W. Chen, C. R. Li, W. H. Tang, ACS Nano **12**(12), 12827 (2018).
[11] K. Balakrishnan, A. Bandoh, M. Iwaya, S. Kamiyama, H. Amano, I. Akasaki, Jpn. J. Appl. Phys. **46**(14), L307 (2007).

[12] M. Imura, K. Nakano, N. Fujimoto, N. Okada, K. Balakrishnan, M. Iwaya, S. Kamiyama, H. Amano, I. Akasaki, T. Noro, T. Takagi, A. Bandoh, Jpn. J. Appl. Phys. **45**(11), 8639 (2006).
[13] W. Yang, S. S. Hullavarad, B. Nagaraj, I. Takeuchi, R. P. Sharma, T. Venkatesan, R. D. Vispute, H. Shen, Appl. Phys. Lett. **82**(20), 3424 (2003).
[14] S. Cui, Z. Mei, Y. Zhang, H. Liang, X. Du, Adv. Opt. Mater. **5**(19), 1700454 (2017).
[15] S. Han, X. Huang, M. Fang, W. Zhao, S. Xu, D. Zhu, W. Xu, M. Fang, W. Liu, P. Cao, Y. Lu, J. Mater. Chem. C **7**(38), 11834 (2019).
[16] Thi Kim Oanh Vu, Dong Uk Lee, Eun Kyu Kim, Nanotechnology **31**(24), 124430 (2020).
[17] Y. Su, Y. Chiou, C. Chang, S. Chang, Y. Lin, J. Chen, Solid-State Electronics **46**(12), 2237 (2002).
[18] T. Oshima, T. Okuno, S. Fujita, Jpn. J. Appl. Phys. **46**(11), 7217 (2007).
[19] T. Oshima, N. Arai, N. Suzuki, S. Ohira S. Fujita, Thin Solid Films **516**(17), 5768 (2008).
[20] K. Sasalo, A. Kuramata, T. Masui, E. G. Vilora, K. Shimamura, S. Yamakoshi, Appl. Phys. Express **5**(3), 035502 (2012).
[21] O. Katz, V. Garber, B. Meyler, G. Bahir, J. Salzman, Appl. Phys. Lett. **79**(10), 1417 (2001).
[22] S. Oh, C. K. Kim, J. Kim, ACS Photonics **5**(3), 1123 (2017).
[23] S. Oh, J. Kim, F. Ren, S. J. Pearton, J. Kim, J. Mater. Chem. C **4**(39), 9245 (2016).
[24] D. Y. Guo, Z. P. Wu, Y. H. An, X. C. Guo, X. L. Chu, C. L. Sun, L. H. Li, P. G. Li, W. H. Tang, Appl. Phys. Lett. **105**(2), 023507 (2014).
[25] D. Y. Guo, H. Z. Shi, Y. P. Qian, M. Lv, P. G. Li, Y. L. Su, Q. Liu, K. Chen, S. L. Wang, C. Cui, C. R. Li, W. H. Tang, Semicond. Sci. Tech. **32**(3), 03LT01 (2017).

*Corresponding author: yuanlei@xidian.edu.cn